Complete functional analysis of type IV pilus components of a reemergent plant pathogen reveals neofunctionalization of paralog genes

Marcus V, Merfa[a], Xinyu Zhu[b], Deepak Shantharaj[a], Laura M. Gomez[a], Eber Naranjo[a], Neha Potnis[a], Paul A. Cobine[b], Leonardo De La Fuente[a]*

[a]Department of Entomology and Plant Pathology, Auburn University, Auburn, AL 36849, USA.

[b]Department of Biological Sciences, Auburn University, Auburn, AL 36849, USA.

*Corresponding author: Leonardo De La Fuente. Mailing address: Department of Entomology and Plant Pathology, 209 Rouse Life Sciences Bldg., Auburn University, Auburn, AL 36849. Phone: (334) 844-2582.

Email: lzd0005@auburn.edu

Abstract

Type IV pilus (TFP) is a multifunctional bacterial structure involved in twitching motility, adhesion, biofilm formation, as well as natural competence. Here, by mutagenesis and functional analysis, we dissected the roles of all genes required for TFP biosynthesis and regulation in the reemergent plant pathogenic fastidious prokaryote *Xylella fastidiosa*. This xylem-limited, insect-transmitted pathogen lives constantly under flow conditions and therefore is highly dependent on TFP for host colonization. In addition, TFP-mediated natural transformation is a process that impacts genomic diversity and environmental fitness. Ten out of the thirty-eight genes analyzed were essential for movement and natural competence. Interestingly, seven sets of paralogs exist, and mutations showed opposing phenotypes, indicating evolutionary neofunctionalization of subunits within TFP. The minor pilin FimT3 was the only protein exclusively required for natural competence. We determined that FimT3 (but not the other two FimT paralogs) is a DNA receptor that is conserved among *X. fastidiosa* strains and binds DNA non-specifically via an electropositive surface. Among plant pathogens, this gene was also found in the genome of strains of the plant associated Xanthomonadaceae family. Overall, we highlight here the complex regulation of TFP in *X. fastidiosa*, providing a blueprint to understand TFP in other bacteria living under flow conditions.

Main

Type IV pili (TFP) are retractable hair-like proteinaceous cell appendages located at one or both poles of a bacterial cell [1]. In addition to playing fundamental roles in twitching motility and natural transformation, they also influence virulence, adhesion, and biofilm formation in many bacterial species [2-4]. During twitching motility, TFP extend, attach to surfaces, then retract pulling cells towards the point of attachment [1,2]. TFP also plays a central part in the DNA-uptake machinery that enables natural transformation [3,5]. Natural transformation is a horizontal gene transfer mechanism that allows bacterial cells to take up free DNA from the environment and incorporate it into their own genomes via homologous recombination (HR) [3,6]. The current model of natural transformation in bacteria involves binding of double-stranded DNA to the tip of TFP, which upon retraction brings this molecule to the outer-membrane surface of the cell [4]. DNA is then transported to the periplasm in a proposed Brownian ratchet mechanism [4,7]. Subsequently, DNA is translocated to the cytosol as a single strand, where recombination occurs if the

60 incoming DNA shares homology with the genome of the recipient cell [3]. Alternatively, the incoming DNA is
61 either metabolized or used as template to repair damaged DNA [8].
62 Natural transformation enables rapid evolution by generating genetic diversity and has been
63 involved in spreading of antibiotic resistance, adaptation to new environments and emergence of
64 pathogens [6,8-10]. In addition to animal pathogens [6,9], natural competence has been detected in two plant
65 pathogens, *Ralstonia solanacearum* [11] and *Xylella fastidiosa* [12], both of which possess a very broad plant
66 host range and are xylem-colonizers[13]. *X. fastidiosa* is a gram-negative fastidious prokaryote that infects
67 and causes reemergent diseases in many economically important crops worldwide, such as grapevine,
68 citrus, almond, peach, blueberry, and olive [14-16]. This pathogen lives constantly under flow conditions
69 inside the xylem of infected plants and the foregut of xylem-feeding insect vectors [17]. The main
70 mechanisms of virulence for *X. fastidiosa* are linked to its ability to move systemically within the xylem by
71 TFP-mediated twitching motility, and formation of biofilm that disrupts sap flow [18].
72 *X. fastidiosa* has been classified into subspecies [19-21], and genome analyses revealed widespread
73 HR events within and among subspecies [21-30]. Moreover, experimental evidence showed that *X. fastidiosa*
74 strains are able to recombine in vitro during coculture of either live or live and dead strains [31]. This
75 process occurs under multiple experimental settings including batch and flow culture conditions with
76 synthetic media or grapevine xylem sap from tolerant and susceptible varieties [12,32,33]. Finally, many of the
77 genes that are undergoing recombination among strains in vitro or in nature, are annotated as having
78 roles in virulence and bacterial fitness[26]. These observations led to the hypothesis that HR, a driver of
79 genetic diversity, is responsible for environmental adaptation [26] and/or host switching/expansion. In fact,
80 intersubspecific HR has been suggested to have a role in plant host expansion by generating strains that
81 infect mulberry [20], citrus, coffee [22], blueberry and blackberry [29].
82 The assembly, function, and regulation of TFP require multiple molecular components. Minor
83 pilins, which are present in much lower quantities than the major pilin, prime the assembly of TFP [34], and
84 some species-specific minor pilins may promote additional functions of TFP, such as aggregation and
85 adherence [35,36]. The functional diversity in pilins is mediated by differences in the C-terminal region of
86 these proteins, since all pilins (including major and minor pilins) share a highly conserved N-terminal
87 region [36]. TFP is key to *X. fastidiosa* in both natural competence, which promotes HR and thus generates

large genetic diversity [26,27,31], and twitching motility[18], which is its only mean of movement and fundamental for a xylem-limited bacterium living under flow conditions. Therefore, in this study we individually assessed the functional role of a comprehensive set of 38 TFP-related genes by site-directed mutagenesis. We identified ten core genes that were essential for both natural competence and movement of this plant pathogen. However, some components, mostly minor pilins, were only essential to one feature or the other, and interestingly most paralogous genes had opposite functions, suggesting neofunctionalization. Additionally, our study identified the FimT3 minor pilin as the DNA receptor of the *X. fastidiosa* pilus. This minor pilin is found among plant pathogens mainly in bacterial species of the Xanthomonadaceae family. Together, our data provide insight into how TFP paralogs evolve to perform specific functions within bacterial cells, and how different bacterial species use unique minor pilins to acquire exogenous DNA through natural competence.

Results

Deletion of TFP-related genes differentially affects natural competence and movement of *X. fastidiosa*. Individual deletion mutant strains were generated by site-directed mutagenesis via natural transformation to determine the functional roles of 38 TFP-related genes (Table S1) [37]. Genes were chosen according to genome annotation and searches based on homology to counterparts encoded by *Pseudomonas aeruginosa* [38,39]. To the best of our knowledge, these genes represent the entire set of TFP genes encoded by *X. fastidiosa* strain TemeculaL. Assessment of natural competence was conducted using the pAX1-Cm plasmid, which recombines into the neutral site 1 of the *X. fastidiosa* genome and inserts a chloramphenicol (Cm) resistance cassette [31,40], whereas twitching motility was determined by measuring colony fringe widths on solid agar plates [41]. Although the knockout of genes studied here did not always modulate natural competence and twitching motility in the same manner, the correlation between these two traits among mutant strains was positive ($R^2 = 0.56$, $P<0.001$; Table S3), indicating that they were usually increased or reduced in a similar manner upon deletion of TFP genes.

A set of ten genes were considered core TFP components as deletion of such genes abrogated both natural competence and movement of *X. fastidiosa* (Fig. 1 and Fig. S1-3). They include the ATPases *pilB* and *pilT*, the prepilin peptidase *pilD*, the TFP assembly platform *pilC*, the whole alignment

116 subcomplex *pilMNOP*, the secretin *pilQ* and the regulatory gene *pilZ*. Deletion of the sensor gene *pilS* of
117 the PilRS two-component regulatory system (Fig. 1 and Fig. S1-3) significantly increased both natural
118 competence and twitching motility, while deletion of the regulator *pilR* was essential for twitching motility
119 but not for transformation. The minor pilin *fimT3* was the only gene found to be essential exclusively for
120 natural competence (Fig. 1 and Fig. S1). Curiously, this Δ*fimt3* strain showed significantly increased
121 twitching motility than wild-type (WT) cells (Fig. 1 and Fig. S2-3).

122 Seven sets of paralogs exist in the *X. fastidiosa* TFP cluster (PilA1-3, PilE/V/W/X1-2, PilY1-3 and
123 FimT1-3). Intriguingly, the knockout of paralogs presented varied phenotypes suggesting duplication and
124 neofunctionalization of the genes. The minor pilins *pilE1V1W1X1*, which are encoded in the same operon
125 (Table S2), were essential for twitching motility but not for transformation (Fig. 1 and Fig. S2-3), although
126 these mutants did show significantly lower recombination frequencies than WT (Fig. 1 and Fig. S1). In
127 comparison to the WT, Δ*pilE2* presented significant higher twitching motility and no changes in natural
128 transformation, Δ*pilV2* had significant higher natural transformation with no altered movement, Δ*pilW2*
129 showed significant higher natural transformation and significant lower movement, and Δ*pilX2* possessed
130 both significant lower natural transformation and twitching motility (Fig. 1 and Fig. S1-3). Knockout of
131 *pilA1* significantly increased both natural competence and twitching motility, whereas deletion of *pilA2* and
132 *pilA3* significantly reduced twitching motility and did not alter natural transformation (Fig. 1 and Fig. S1-3).
133 A strain with deletion of both *pilA1* and *pilA2* abolished twitching motility (Fig. 1 and Fig. S2-3), as
134 described elsewhere [37]. Additionally, deletion of the minor pilin *fimT1* significantly decreased both natural
135 competence and movement, while knockout of *fimT2* significantly increased natural competence and did
136 not change twitching motility, and Δ*fimT3* lost natural competence and presented significantly higher
137 movement than the WT (Fig. 1 and Fig. S1-3). As for *pilY1-1*, *pilY1-2* and *pilY1-3*, which are tip adhesins,
138 their deletion significantly reduced twitching motility. However, Δ*pilY1-1* and Δ*pilY1-2* presented
139 significant lower natural competence whilst Δ*pilY1-3* had significant higher natural competence than the
140 WT (Fig. 1 and Fig. S1-3).

141 Lastly, deletion of the pilotin *pilF* and of the retraction ATPase *pilU* significantly reduced natural
142 competence and movement. Knockout of the chemotaxis genes *pilGHIJL* and *chpBC* significantly
143 reduced twitching. However, Δ*pilG*, Δ*pilH* and Δ*pilL* showed increased natural competence, while Δ*pilJ*

and Δ*chpC* had lower natural competence, and Δ*pilI* and Δ*chpB* did not change this phenotype in comparison to the WT (Fig. 1 and Fig. S1-3).

TFP-related genes differentially modulate other virulence traits of *X. fastidiosa*. We evaluated phenotypes such as growth, biofilm formation, cell aggregation (measured by settling rate), and virulence in planta of the individual TFP mutants. Growth rates were measured by change in OD_{600nm} over time (Fig. S4-S5). Since this growth analysis considered only turbidity that may be affected by cell attachment (biofilm) to surfaces and cell-to-cell aggregation, the number of viable *X. fastidiosa* cells (measured as CFU/ml) was also evaluated. Only the non-recombinant and non-motile Δ*pilC* and Δ*pilP* mutants showed significant changes in the number of cells in comparison to WT, with both having significantly higher populations (Fig. S6). Biofilm formation is a critical aspect of virulence in *X. fastidiosa*. Individual deletion of *pilB*, *pilD*, *pilH*, *pilI*, *pilM*, *pilN*, *pilO*, *pilQ*, *pilR*, *pilT*, *pilX1* and *fimT1* significantly increased biofilm formation, whereas Δ*pilA3* and Δ*fimT3* formed significant less biofilm than WT (Fig. S7). Planktonic growth was significantly increased for strains with individual deletion of *pilA1*, *pilC*, *pilE1*, *pilF*, *pilM*, *pilN*, *pilO*, *pilP*, *pilQ*, *pilR*, *pilV1*, *pilW1*, *pilW2*, *pilX1*, *pilA1pilA2*, *pilY1-1*, *fimT3* and *chpC*, while individual knockout of *pilD*, *pilT* and *pilY1-3* significantly decreased planktonic growth (Fig. S8). Moreover, only Δ*pilD*, Δ*pilT* and Δ*pilX2* showed significant higher settling rates, with other mutants not differing significantly from the WT (Fig. S9). Biofilm formation and settling rate, as well as planktonic growth and growth rate were positively correlated (Table S3). Meanwhile, biofilm formation and twitching motility/growth rate, settling rate and planktonic growth/growth rate, and growth rate and total viable *X. fastidiosa* had significant negative correlations (Table S3). No other phenotype presented a significant correlation to recombination frequency besides twitching motility.

Virulence of a subset of the *X. fastidiosa* mutant strains was assessed by inoculating *Nicotiana tabacum* L. cv. Petite SR1 plants and scoring disease incidence and severity. Mutants chosen for analysis had different twitching motility phenotypes, such as higher movement (Δ*pilA1* and Δ*pilS*), lower movement (Δ*pilA2*) and non-motility (Δ*pilA1pilA2*, Δ*pilQ* and Δ*pilR*). Additionally, mutants in the DNA-binding *fimT3* (see below) and the paralogs *fimT1* and *fimT2* were tested and no significant change in virulence was found compared to WT (data not shown). WT-inoculated plants presented the highest

disease severity over the time course of assays (Fig. S10a), with all plants inoculated with the mutant strains having significantly lower AUDPC (Area Under the Disease Progress Curve) values, except plants inoculated with Δ*pilA2* (Fig. S10b). All inoculated plants reached 100% disease incidence at the end of assays, except plants inoculated with Δ*pilA1*, which had 89% disease incidence (±11%, standard error). However, only WT-inoculated plants consistently presented severe symptoms of leaf scorch, while plants inoculated with the mutant strains mostly presented mild symptoms (Fig. S10d). In addition, when evaluating the population of *X. fastidiosa* in planta by qPCR, only the Δ*pilA1pilA2* double mutant showed a defect in colonizing the top leaf of the plant host, and the Δ*pilQ* and Δ*pilR* mutants presented significant higher population in the basal leaf of plant hosts (Fig. S10c). Together, results demonstrate that the deletion of analyzed genes significantly reduced symptoms development in infected tobacco plants (except for deletion of *pilA2*), which was not explained by bacterial distribution, since most strains could effectively colonize the entirety of plants (except Δ*pilA1pilA2*).

The minor pilin FimT3 is the DNA receptor of the *X. fastidiosa* type IV pilus. The observation of the minor pilin FimT3 being the only TFP component that is essential exclusively for natural transformation (Fig.1 and Fig. S1-3) led us to hypothesize that this component is the DNA receptor of the TFP of *X. fastidiosa*. We first analyzed the piliation phenotype of Δ*fimT3* in comparison to WT by transmission electron microscopy (TEM). Both presented long TFP as well as short type I pili, with no apparent changes in the piliation of *X. fastidiosa* cells upon deletion of *fimT3* (Fig. 2a). Next, the ability of these cells to take up DNA from the extracellular environment was evaluated by exposing them to Cy-3-labeled pAX1-Cm plasmid and observing under a fluorescent microscope. After exposure to the fluorescently labeled DNA fragment, WT cells imported DNA allowing for protection from exogenous DNaseI, but no fluorescent DNA foci were present in Δ*fimT3* cells (Fig. 2b). DNA foci were mostly observed at one pole of the cells, which coincides to the described phenotype of *X. fastidiosa* that forms TFP at only one of its poles [42]. The DNA-uptake ability of the mutant strains of other minor pilins that decreased the natural transformation ability of *X. fastidiosa* upon deletion was also evaluated for comparison. These included Δ*pilE1*, Δ*pilV1*, Δ*pilW1*, Δ*pilX1*, Δ*pilX2*, Δ*fimT1* and Δ*fimT2* (Fig.1 and Fig. S1). The Δ*fimT2* mutant strain was included because this gene is a paralog of *fimT3*, even though its

200 deletion increased the natural competence of *X. fastidiosa* (Fig.1 and Fig. S1). All analyzed mutant strains
201 maintained the DNA-uptake (competence) phenotype (Fig. S11), but at different levels (Fig. S12). WT
202 cells presented the highest percentage of cells with DNA foci, with Δ*pilE1* having the lowest proportion of
203 cells with DNA acquisition (Fig. S12).

204 To determine the DNA-binding ability of FimT3, and compare to its paralogs FimT1 and FimT2,
205 the soluble portion of these proteins (named FimT3s, FimT1s and FimT2s, respectively), which lacked the
206 conserved N-terminal hydrophobic α-helices of pilins [36], were amplified and cloned for expression. These
207 proteins were then purified and assayed for DNA binding by agarose electrophoretic mobility shift assay
208 (EMSA). Results showed FimT3s was the only protein capable of binding DNA, since no shift was
209 observed with FimT1s and FimT2s when using as much as 10 μM of each protein (Fig. 2c). Moreover,
210 FimT3s was able to bind to different DNA sequences, independent of homology to the *X. fastidiosa*
211 TemeculaL genome, indicating that binding is not sequence-specific (Fig. S13). Collectively, *fimT3* being
212 the only gene essential exclusively for natural competence, the ability of FimT3 to bind to DNA and the
213 loss of DNA acquisition from the extracellular environment by cells upon its deletion, demonstrate that this
214 minor pilin is the DNA receptor of the *X. fastidiosa* TFP.

215 To further characterize FimT3, we searched for specific amino acid residues involved in DNA-
216 binding. The binding of DNA to TFP via a minor pilin was demonstrated in ComP of *Neisseria,* ComZ of
217 *Thermus thermophilus,* and VC0858 of *Vibrio cholerae* [4,43,44]. Amino acids alignments revealed that
218 FimT3 and ComP share only 28% identity (64% similarity) over 20% of query sequence, while FimT3 and
219 ComZ have no significant identity. Alignment of FimT3 with VC0858 of *Vibrio cholerae* showed 35%
220 identity and 62% similarity over 18% of query sequence. In spite of the low overall homology the
221 sequence alignments showed that an arginine residue at position 162 of FimT3 aligned with a lysine of
222 ComP (K108) that was previously demonstrated to be essential for its DNA-binding ability [43] (Fig. S14a).
223 Additionally, an arginine residue at position 160 of FimT3 aligned with an arginine of VC0858 (R168) that
224 was also important for the DNA-binding activity of the *V. cholerae* pilus [4] (Fig. S14b). These two arginine
225 residues of FimT3 (R160 and R162) were predicted in silico to have the highest probabilities of binding
226 DNA among the residues of this protein (Table S4). Moreover, alignment of FimT3 with a FimT ortholog
227 that is essential for natural competence of *Acinetobacter baylyi* [45] (28% identity and 46% similarity over

91% of query sequence) showed alignment of R162 of FimT3 to an arginine of FimT from *A. baylyi*. Likewise, FimT3 shares 27% identity (48% similarity) over 80% of query sequence with a recently described DNA-binding FimT ortholog of *Legionella pneumophila*, in which the aligned R160 and R162 have been demonstrated as important to bind DNA [46] (Fig. S14c).

Analysis of a structural model produced by the Phyre2 algorithm, showed that R160 and R162 of FimT3 are located within an electropositive surface and could form a pocket to bind DNA (Fig. 2d). Thus, to assess the role of these arginine residues in the DNA-binding ability of FimT3, we generated a FimT3s variant by site-directed mutagenesis in which both arginine residues were replaced by alanine residues (FimT3s-R160AR162A). Agarose EMSAs revealed that WT-FimT3s had a higher affinity for DNA than FimT3s-R160AR162A based on the amount of protein needed to shift 50% of the input DNA (Fig. 2e). Similar results were obtained when using the more sensitive acrylamide EMSA and the kanamycin (Km) resistance cassette sequence as target DNA (previously determined to be bound by FimT3s in Fig. S13). An abrupt shift was detected when using concentrations of FimT3s ranging between 1 and 5 μM, whereas a much more subtle and gradual shift was observed for samples treated with FimT3s-R160AR162A within the same concentration range (Fig. 2f). We then performed a densitometry analysis of the shifted bands treated with concentrations ranging between 1 and 10 μM of each protein (Fig. 2g) and calculated the area under the curve to quantify the DNA-binding affinity of FimT3s and FimT3s-R160AR162A. While the DNA-binding affinity of FimT3s-R160AR162A was lower than that of FimT3s (Fig. 2h), the mutations did not completely abolish DNA-binding ability suggesting other residues are contributing to this activity. Nonetheless, these results show that R160 and R162 are important for DNA-binding activity of FimT3.

FimT3 is widely conserved within *X. fastidiosa* strains and, among plant pathogens, is encoded by other members of the Xanthomonadaceae family. Previously, DNA-binding homologues of FimT3 have been found in many representative species of γ-Proteobacteria, including the Xanthomonadaceae family to which *X. fastidiosa* belongs [46]. We performed searches using the Conditional Reciprocal Best BLAST (CRB-BLAST) [47], as well as phylogenetic analyses, to further explore the distribution of the *fimT* paralogs within this family. All three paralogs of *fimT* are encoded by *X. fastidiosa*, *X. taiwanensis*, many clade II *Xanthomonas* spp.[48] and few *Pseudoxanthomonas* spp. (Fig. 3).

Curiously, early branching clade I *Xanthomonas* spp. only encode *fimT1* and *fimT3* (Fig. 3). Specifically, *fimT3* was present in 1,416 out of 3,001 genomes of the Xanthomonadaceae (47%), majority of them belonging to species within the genus *Xanthomonas*. In the *fimT3* clade, *X. fastidiosa* strains grouped together, including *X. taiwanensis*, with a similar trend being observed for *Xanthomonas* spp. strains (Fig. 3). However, clade I and clade II *Xanthomonas* spp. and other Xanthomonadaceae species clustered mostly separated (Fig. 3). The alignment of the different FimT3 sequences encoded by *X. fastidiosa* strains showed a maximum of six nonconservative substitutions within strains belonging to the subspecies *pauca*, which encode FimT3 that are 13 amino acids shorter than other strains (Fig. S15a). Alignment of representative FimT3 sequences among strains belonging to the Xanthomonadaceae family revealed that the arginine residues at positions 160 and 162 of FimT3 from *X. fastidiosa* strain TemeculaL were conserved in most orthologous sequences of this protein (Fig. S15b). Additionally, R160 was always preceded by a glycine residue, constituting a highly conserved GRxR motif (Fig. S15b), as seen elsewhere [46]. Although amino acid identities ranged from 95.60% to 100% within *X. fastidiosa*, and from 15.5% to 80% compared to other species, only 41 out of 1,416 FimT3 sequences encoded by the Xanthomonadaceae do not carry the GRxR motif (Table S5). Overall, results indicate that FimT3 is encoded by representative plant pathogens of the Xanthomonadaceae and that R160 and R162 are highly conserved within FimT3 sequences.

Discussion

In this study we defined the roles of individual subunits involved in regulation, assembly, and functioning of the *X. fastidiosa* TFP on natural competence, twitching motility, adhesion, and biofilm (Fig. 4). To our knowledge, our study comprises the largest simultaneous functional description of a comprehensive set of TFP-related genes. By performing site-directed mutagenesis of all TFP genes followed by functional studies, we defined a set of ten core genes (*pilBCDMNOPQTZ*) that were essential for natural competence and movement. Most of these proteins are inner- or outer-membrane associated, confirming the important role of membrane anchorage for functionality of TFP.

283 Collectively, our data highlight the pervasive neofunctionalization among TFP components since
284 seven paralogous gene sets exerted mainly opposing regulatory functions on movement and natural
285 competence. For instance, paralogs of the minor pilins *pilEVWX* and *fimT* and the TFP tip adhesin *pilY1*
286 are mostly organized as operons in two different regions of the *X. fastidiosa* TemeculaL genome (Table
287 S2). Here, we observed that individual mutations in one set of these paralogs abrogated twitching motility
288 and greatly reduced natural competence, while deletions in the other set of paralogous genes produced
289 variable phenotypes that were mostly opposite to their counterparts. It has been demonstrated that minor
290 pilins prime the assembly of TFP [34]. This interaction is specific, in which major pilins require a specific
291 cognate subset of minor pilins for TFP assembly [49]. Therefore, the presence of paralogs for major and
292 minor pilins displaying opposite functions within *X. fastidiosa* possibly suggest assembly of multiple TFP
293 fibers with specific functions. However, this needs to be further assessed (see SI discussion).
294 Most remarkably among paralogs, is the discovery of the minor pilin FimT3 as the TFP DNA receptor.
295 This is an outstanding neofunctionalization example since FimT1 and FimT2 did not show DNA
296 adherence abilities. This finding was also supported by our phylogenetic analysis, which showed
297 divergent evolution of FimT3 from its paralogs. FimT3 plays an essential role in natural competence by
298 mediating extracellular DNA uptake that may be integrated into the genome, thereby conferring new
299 phenotypic traits that may allow an increase in bacterial fitness and/or host expansion of *X. fastidiosa*.
300 The interaction between DNA molecules and an extracellular specific receptor is a key first step in the
301 DNA uptake and thus natural competence of bacterial species. Initially, DNA binding by TFP has been
302 observed in *P. aeruginosa* [50], *Streptococcus pneumoniae* [51], and *V. cholerae* [4], in which pilus retraction
303 drives DNA uptake by transporting it to the cell surface, which is then imported to the periplasm by the
304 competence protein ComEA [4,7]. Although these early studies provide evidence that the specialized DNA
305 receptor resides within type IV competence pilus fibers, no direct binding of DNA by individual purified
306 major and/or minor pilins was reported. In *V. cholerae*, targeted mutations of positively charged amino
307 acid residues within the minor pilins VC0858 and VC0859 reduced the DNA-binding affinity of its TFP [4],
308 but the ability of these minor pilins to directly bind DNA was not assayed. Direct DNA binding has been
309 first observed for the pilin protein ComP from *N. meningitidis*, with binding occurring at a positively
310 charged surface of this protein [43]. ComP orthologs are found mostly within the Neisseriaceae family,

311 where they mediate DNA uptake by binding to specific DNA uptake sequences, as *Neisseria* spp.
312 preferentially take up homotypic DNA [43,52]. ComZ, encoded by *T. thermophilus*, was the second minor
313 pilin described as a TFP DNA receptor [44]. However, ComZ is an unusual minor pilin that possesses an
314 additional large β-solenoid domain inserted into the common β-sheet structure of pilins. Furthermore,
315 ComZ binds to another minor pilin, PilA2 (PilV in *X. fastidiosa*), and its DNA binding ability does not
316 appear to require positive charges in its surface [44]. Nonetheless, the binding of ComZ to another minor
317 pilin suggests that specific interactions within the pilus structure may occur to assemble the competence
318 pilus fiber.

319 Here, the deletion of individual paralogs of the major pilin PilA abrogated neither natural
320 competence nor twitching motility, suggesting functional overlapping among them (see SI Discussion). In
321 addition to the novel functions described above, our study confirmed the role of core components that
322 were previously analyzed in other bacterial species including *Acinetobacter baumannii* [53], *A. baylyi* [45], *T.*
323 *thermophilus* [54], *Haemophilus influenzae* [55], *P. aeruginosa* [56-59], *L. pneumophila*[46] and *X. fastidiosa* [32,42,60].
324 The exceptions were *pilP* and *pilZ* in which previous deletion of both greatly reduced natural competence
325 [61,62], but did not abolish it here. It is of note that very few of these genes have been simultaneously
326 assayed for their role in both natural transformation and movement mediated by TFP.

327 Deletion of FimT3 in *X. fastidiosa*, but not of the paralogs FimT1 and FimT2, exclusively disrupted
328 the natural competence of this bacterium. FimT3 binds to DNA via a surface in which positively charged
329 arginine residues contribute to the DNA binding ability of this protein. However, the binding appears to be
330 non-specific, which is in contrast to ComP [43]. FimT from the human pathogen *L. pneumophila* [46], which is
331 a homologue of the FimT3 studied here, was recently identified as a pilin with DNA-binding ability.
332 Another FimT homolog was also demonstrated to be specialized in natural competence in *A. baylyi* [45],
333 although no DNA binding was assessed. In our study, FimT3 seems to be particularly enriched in plant
334 pathogens of the Xanthomonadaceae family, being encoded by all *X. fastidiosa* strains as well as many
335 other bacterial species belonging to this family. Thus, our results, together with previous studies,
336 demonstrate that DNA binding by TFP occurs among bacterial species through a similar component such
337 as minor pilins, which themselves are not widely distributed or conserved, but are rather specific to
338 different bacterial groups. For instance, the ability of strain-specific subsets of minor pilins to modulate

TFP dynamics has already been described in *P. aeruginosa* (see SI Discussion) [49]. Understanding how this minor pilin interacts with different minor and major pilins of *X. fastidiosa* in the competence pilus is an important area to explore. It is not known whether the other Xanthomonadaceae bacterial species encoding FimT3 that were found in our analysis are also naturally competent. For instance, *X. fastidiosa* strains belonging to the *pauca* subspecies have a shorter FimT3 amino acid sequence, missing part of the C-terminal, and have a few aminoacidic changes (although maintain the arginine residues studied here). The only reported attempt to transform a *X. fastidiosa* strain belonging to the subspecies *pauca* by natural competence in vitro has failed [63]. Studies with the *X. fastidiosa* subsp. *pauca* FimT3 variant should investigate both individual DNA-binding activity and potential roles of the C-terminus in interaction with the rest of the TFP structure.

In summary, our study highlights the fundamental functions of TFP in virulence and evolution evidenced by complex regulatory features. Due to the worldwide threat that *X. fastidiosa* presents to many economically important crops and to the ever-increasing list of plant hosts, it is imperative to investigate how this plant pathogen acquires foreign DNA and expands its genetic diversity to help researchers understand its eco-evolutionary history and re-emergence of this pathogen in many geographic areas. In addition, our results provide a robust blueprint to assess TFP functions in bacteria living under flow conditions. An extensive discussion including additional genes analyzed in this study and their functional roles in natural transformation and twitching motility of *X. fastidiosa*, in addition to unique behaviors and other phenotypes such as biofilm formation, virulence in planta, and diversity in paralogous genes functions, is included in SI Discussion. All of this indicates that a complex and tightly regulated machinery is involved in these bacterial functions.

Methods

Methods that are only cited here are described in detail in SI Materials and Methods.

Bacterial strains, plasmids, and culture conditions. All strains and plasmids used in this study are listed in Table S6. All *X. fastidiosa* mutant strains used here are derivatives of the *X. fastidiosa* subsp. *fastidiosa* strain TemeculaL [26], and were originated by site-directed mutagenesis of each gene of interest

using natural competence as described elsewhere [37]. Primers used in this process are listed in Table S7. *X. fastidiosa* was recovered from -80 ºC glycerol stocks and routinely cultured for seven days at 28 ºC on periwinkle wilt (PW) agar plates [64], modified by removing phenol red and using bovine serum albumin (1.8 g/l) (BSA; Gibco Life Sciences Technology), and sub-cultured onto fresh PW agar plates for another seven days at 28 ºC before use. *X. fastidiosa* mutant strains were grown similarly but using PW plates amended with Km. All assays were performed using the subcultured *X. fastidiosa* strains. Cells were suspended and cultured in PD3 broth [64] to perform phenotypic assays, while phosphate-buffered saline (PBS) was used to suspend cells in liquid for in planta assays. Whenever needed, the antibiotics Km and Cm were used at concentrations of 50 and 10 µg/ml, respectively. When used together with Cm, the Km concentration was reduced to 30 µg/ml. Luria-Bertani (LB) medium (BD Difco) was used to culture *E. coli* cells. When needed, Km, Cm and ampicillin (Amp) were added to LB at concentrations of 50, 35 and 100 µg/ml, respectively.

Phenotypic analyses of *X. fastidiosa* WT and mutant strains. Analyses of natural competence among strains [31], twitching motility [33], growth curve and growth rate [31], biofilm formation and planktonic growth [31,65], settling rate [31], piliation observation by TEM [37], and virulence in planta using tobacco as model system [66] were performed as described elsewhere. All experiments had at least three biological replicates, unless otherwise stated.

DNA uptake assays. DNA uptake assays were performed as similarly described for the analysis of natural competence among *X. fastidiosa* strains (see SI Materials and Methods). Briefly, recipient cells were suspended in PD3 broth to OD_{600nm} = 0.6, spotted onto PD3 agar plates and grown for three days at 28 ºC. Then, 1 µg of fluorescently labeled pAX1-Cm plasmid (10-µl volume), labeled using the *Label* IT Nucleic Acid Labeling kit, Cy3 (Mirus Bio LLC), was added on top of cells, air-dried, and incubated at 28 ºC for another 24 h. After, cells were harvested in 150 µl of PD3 broth, and a 50 µl aliquot was treated with 10 units of DNase I (New England Biolabs) for 10 minutes at 37 ºC to degrade the remaining extracellular DNA, and cells were observed using a 100× oil immersion objective in a Nikon Eclipse Ti inverted microscope (Nikon). Image acquisition was performed using a Nikon DS-Q1 digital camera

395 (Nikon) controlled by the NIS-Elements software version 3.0 (Nikon), which was also used to create
396 merged fluorescent images. To detect Cy3, an excitation wavelength of 590 nm was used (tetramethyl
397 rhodamine isothiocyanate; TRITC filter). The proportion of cells that acquired extracellular DNA was
398 calculated as the percentage of cells with fluorescent DNA foci to cells without fluorescent DNA foci.
399 Experiments were performed at least three times independently.
400
401 **Protein cloning, expression, and purification.** Cloning, expression, and purification of FimT1s,
402 FimT2s and FimT3s were performed similarly as described elsewhere using the pHIS-Parallel1 plasmid
403 (Table S6) [67,68]. Amino acid exchanges in FimT3s were performed by designing a pair of primers (Table
404 S7) that exchanged the arginine residues at positions 160 and 162 by alanine residues. This pair of
405 primers was designed using the QuickChange Primer Design tool (Agilent Technologies, Inc.;
406 https://www.agilent.com/store/primerDesignProgram.jsp). For amino acid exchanges, the whole pHIS-
407 Parallel1-*fimT3s* construct was amplified via *Pfu* DNA polymerase (G-Biosciences) using a standard
408 protocol from the manufacturer and this pair of primers in a S1000 thermal cycler (Bio-Rad). Expression
409 and purification of FimT3s-R160AR162A were performed as described above (see SI Materials and
410 Methods) [67]. PCR products were purified using the Gel/PCR DNA Fragments Extraction kit (IBI Scientific).
411 Correct cloning and amino acid exchanges in all constructs were confirmed by Sanger sequencing
412 (Sequetech Corporation) using the T7 promoter forward primer (Table S7).
413
414 **DNA binding assays.** Agarose EMSAs were mainly performed to assess the DNA-binding ability
415 of purified FimT1s, FimT2s and FimT3s. Briefly, 200 ng of DNA (usually pAX1-Cm plasmid) were
416 incubated for 30 minutes at 28 ºC with increasing concentrations of purified proteins in 20 µL EMSA
417 reaction buffer (50 mM Tris-HCl, pH 7.5; 50 mM NaCl; 200 mM KCl; 5 mM $MgCl_2$; 5 mM EDTA, pH 8.0; 5
418 mM DTT; 0.25 mg/ml BSA). Lysis buffer containing 250 µM imidazole, in which proteins were suspended,
419 was included as blank control. After the incubation period, DNA was separated by electrophoresis on a
420 0.8% agarose gel containing GelRed nucleic acid gel stain (Biotium) in Tris-acetate-EDTA buffer (120 V
421 for 40 minutes). Experiments were performed at least three times independently. On the other hand,
422 native acrylamide EMSAs were used to perform titration of the DNA binding activity of FimT3s and

FimT3s-R160AR162A. In summary, 60 ng of Cy-3 labeled Km resistance cassette were incubated for 30 minutes at 28 ºC with increasing concentrations of purified proteins in 20 µL EMSA reaction buffer and separated by electrophoresis on a 3.5% native acrylamide gel in Tris-borate-EDTA buffer (40 V for 4 hours). Native acrylamide gels were pre-run at 40 V for 30 minutes before being used. DNA samples were directly visualized using the ImageQuant LAS 4010 Imaging System (GE Healthcare), since the used DNA was fluorescently labeled with Cy3. Experiments were performed two times independently. Densitometry analysis of the shifted bands of Cy-3 labeled DNA in native acrylamide gels was performed by measuring the fluorescent intensity of these bands when treated with 1, 2, 5, and 10 µM of each protein using ImageJ [69]. Then, these values were used to calculate the area under the fluorescent curves, as performed to obtain the AUDPC (see SI Materials and Methods) [70], to quantify the DNA-binding affinity of FimT3s and FimT3s-R160AR162A by determining the progress of shifted bands in relation to each protein concentration.

Bioinformatic analyses. FimT3 modeling was performed using the Phyre2 web portal [71] and visualized via PyMOL version 2.4.0 (Schrödinger, LLC). The surface electrostatics of FimT3 was predicted using the APBS Electrostatics plugin from PyMOL. Sequence alignments of FimT3 with ComP, VC0858 and FimT from *A. baylyi* and *L. pneumophila* were performed by retrieving the respective sequences from NCBI, aligning through the T-Coffee Multiple Sequence Alignment Server [72] and visualizing using the BoxShade webserver (https://embnet.vital-it.ch/software/BOX_form.html). For FimT3 analyses within the Xanthomonadaceae family, DNA sequences of different FimT homologs from *Xylella*, *Xanthomonas*, *Lysobacter* and *Stenotrophomonas* were used as query for screening genomes of Xanthomonadaceae using CRB-BLAST [47] with default settings. Nucleotide sequences for the CRB-BLAST hits were then retrieved and aligned using MAFFT [73], followed by RAxML version 8.0.24 [74] to build a phylogenetic tree, which was visualized using FigTree version 1.4.4 (http://tree.bio.ed.ac.uk/). FimT3-encoding sequences were retrieved from the phylogenetic tree using the TREE2FASTA Perl script [75], translated into amino acid sequences and aligned using Clustal Omega (Clustal 12.1) to determine percentage of identical amino acids [76]. The visualization of the alignment of representative FimT3 sequences among *X. fastidiosa* strains and representative bacterial species belonging to the

Xanthomonadaceae family was performed using the BoxShade webserver. The FimT3 GRxR motif sequence logo was generated using the WebLogo webserver[77].

Data analysis. Data from natural competence assays (recombination frequency) and the area under the fluorescent curve were compared by two-tailed Student's *t*-test. Data from twitching motility, growth rate, viable *X. fastidiosa* CFU/ml obtained during natural competence assays, biofilm formation, planktonic growth, settling rate, AUDPC, *X. fastidiosa* population in planta and percentage of cells acquiring DNA from the extracellular environment were individually analyzed by one-way analysis of variance (ANOVA) followed by Tukey's HSD multiple comparisons of means in R 4.0.0 under the package multcomp [78]. Correlation among analyzed phenotypes was determined by Pearson's correlation using the SigmaPlot software version 11.0 (Systat Software Inc.).

References

1 Mattick, J. S. Type IV pili and twitching motility. *Annu Rev Microbiol* **56**, 289-314, doi:10.1146/annurev.micro.56.012302.160938 (2002).

2 Jarrell, K. F. & McBride, M. J. The surprisingly diverse ways that prokaryotes move. *Nat Rev Microbiol* **6**, 466-476 (2008).

3 Dubnau, D. & Blokesch, M. Mechanisms of DNA uptake by naturally competent bacteria. *Annu Rev Genet* **53**, 217-237, doi:10.1146/annurev-genet-112618-043641 (2019).

4 Ellison, C. K. *et al.* Retraction of DNA-bound type IV competence pili initiates DNA uptake during natural transformation in *Vibrio cholerae*. *Nat Microbiol* **3**, 773-780, doi:10.1038/s41564-018-0174-y (2018).

5 Seitz, P. & Blokesch, M. DNA-uptake machinery of naturally competent *Vibrio cholerae*. *Proc Natl Acad Sci U S A* **110**, 17987-17992, doi:10.1073/pnas.1315647110 (2013).

6 Johnston, C., Martin, B., Fichant, G., Polard, P. & Claverys, J. P. Bacterial transformation: distribution, shared mechanisms and divergent control. *Nat Rev Microbiol* **12**, 181-196 (2014).

7 Seitz, P. *et al.* ComEA is essential for the transfer of external DNA into the periplasm in naturally transformable *Vibrio cholerae* cells. *PLoS Genet* **10**, e1004066, doi:10.1371/journal.pgen.1004066 (2014).

8 Seitz, P. & Blokesch, M. Cues and regulatory pathways involved in natural competence and transformation in pathogenic and environmental Gram-negative bacteria. *FEMS Microbiol Rev* **37**, 336-363, doi:10.1111/j.1574-6976.2012.00353.x (2013).

9 Johnsborg, O., Eldholm, V. & Håvarstein, L. S. Natural genetic transformation: prevalence, mechanisms and function. *Res Microbiol* **158**, 767-778, doi:10.1016/j.resmic.2007.09.004 (2007).

10 Wiedenbeck, J. & Cohan, F. M. Origins of bacterial diversity through horizontal genetic transfer and adaptation to new ecological niches. *FEMS Microbiol Rev* **35**, 957-976, doi:10.1111/j.1574-6976.2011.00292.x (2011).

11 Bertolla, F., Frostegård, Å., Brito, B., Nesme, X. & Simonet, P. During infection of its host, the plant pathogen *Ralstonia solanacearum* naturally develops a state of competence and exchanges genetic material. *Mol Plant Microbe Interact* **12**, 467-472 (1999).

12 Kung, S. H. & Almeida, R. P. P. Natural competence and recombination in the plant pathogen *Xylella fastidiosa*. *Appl Environ Microbiol* **77**, 5278-5284, doi:10.1128/AEM.00730-11 (2011).

13 De La Fuente, L., Merfa, M. V., Cobine, P. A. & Coleman, J. J. Pathogen adaptation to the xylem environment. *Annu Rev Phytopathol* **60**, 8.1-8.24, doi:10.1146/annurev-phyto-021021-041716 (2022).
14 Hopkins, D. L. & Purcell, A. H. *Xylella fastidiosa*: Cause of Pierce's Disease of grapevine and other emergent diseases. *Plant Dis* **86**, 1056-1066 (2002).
15 Saponari, M., Boscia, D., Nigro, F. & Martelli, G. P. Identification of DNA sequences related to *Xylella fastidiosa* in oleander, almond and olive trees exhibiting leaf scorch symptoms in Apulia (Southern Italy). *J. Plant Pathol.* **95**, 668 (2013).
16 Chang, C. J., Donaldson, R., Brannen, P., Krewer, G. & Boland, R. Bacterial leaf scorch, a new blueberry disease caused by *Xylella fastidiosa*. *HortScience* **44**, 413-417 (2009).
17 Almeida, R. P. P., Coletta-Filho, H. D. & Lopes, J. R. S. in *Manual of Security Sensitive Microbes and Toxins* (ed D. Liu) 841-850 (CRC Press, 2014).
18 Chatterjee, S., Almeida, R. P. P. & Lindow, S. Living in two worlds: the plant and insect lifestyles of *Xylella fastidiosa*. *Annu Rev Phytopathol* **46**, 243-271, doi:10.1146/annurev.phyto.45.062806.094342 (2008).
19 Schaad, N. W., Postnikova, E., Lacy, G., Fatmi, M. & Chang, C. J. *Xylella fastidiosa* subspecies: *X. fastidiosa* subsp. [correction] *fastidiosa* [correction] subsp. nov., *X. fastidiosa* subsp. *multiplex* subsp. nov., and *X. fastidiosa* subsp. *pauca* subsp. nov. *Syst Appl Microbiol* **27**, 290-300, doi:10.1078/0723-2020-00263 (2004).
20 Nunney, L., Schuenzel, E. L., Scally, M., Bromley, R. E. & Stouthamer, R. Large-scale intersubspecific recombination in the plant-pathogenic bacterium *Xylella fastidiosa* is associated with the host shift to mulberry. *Appl Environ Microbiol* **80**, 3025-3033, doi:10.1128/AEM.04112-13 (2014).
21 Scally, M., Schuenzel, E. L., Stouthamer, R. & Nunney, L. Multilocus sequence type system for the plant pathogen *Xylella fastidiosa* and relative contributions of recombination and point mutation to clonal diversity. *Appl Environ Microbiol* **71**, 8491-8499, doi:10.1128/AEM.71.12.8491-8499.2005 (2005).
22 Nunney, L., Yuan, X., Bromley, R. E. & Stouthamer, R. Detecting genetic introgression: high levels of intersubspecific recombination found in *Xylella fastidiosa* in Brazil. *Appl Environ Microbiol* **78**, 4702-4714, doi:10.1128/AEM.01126-12 (2012).
23 Almeida, R. P. P. *et al.* Genetic structure and biology of *Xylella fastidiosa* strains causing disease in citrus and coffee in Brazil. *Appl Environ Microbiol* **74**, 3690-3701, doi:10.1128/AEM.02388-07 (2008).
24 Coletta-Filho, H. D., Francisco, C. S., Lopes, J. R. S., Muller, C. & Almeida, R. P. P. Homologous recombination and *Xylella fastidiosa* host-pathogen associations in South America. *Phytopathology* **107**, 305-312, doi:10.1094/PHYTO-09-16-0321-R (2017).
25 Nunney, L. *et al.* Population genomic analysis of a bacterial plant pathogen: novel insight into the origin of Pierce's disease of grapevine in the U.S. *PLoS One* **5**, e15488, doi:10.1371/journal.pone.0015488 (2010).
26 Potnis, N. *et al.* Patterns of inter- and intrasubspecific homologous recombination inform eco-evolutionary dynamics of *Xylella fastidiosa*. *ISME J* **13**, 2319-2333, doi:10.1038/s41396-019-0423-y (2019).
27 Vanhove, M. *et al.* Genomic diversity and recombination among *Xylella fastidiosa* subspecies. *Appl Environ Microbiol* **85**, e02972-02918, doi:10.1128/AEM (2019).
28 Castillo, A. I., Chacón-Díaz, C., Rodríguez-Murillo, N., Coletta-Filho, H. D. & Almeida, R. P. P. Impacts of local population history and ecology on the evolution of a globally dispersed pathogen. *BMC Genomics* **21**, 369, doi:10.1186/s12864-020-06778-6 (2020).
29 Nunney, L., Hopkins, D. L., Morano, L. D., Russell, S. E. & Stouthamer, R. Intersubspecific recombination in *Xylella fastidiosa* strains native to the United States: infection of novel hosts associated with an unsuccessful invasion. *Appl Environ Microbiol* **80**, 1159-1169, doi:10.1128/AEM.02920-13 (2014).
30 Jacques, M. A. *et al.* New coffee plant-infecting *Xylella fastidiosa* variants derived via homologous recombination. *Appl Environ Microbiol* **82**, 1556-1568, doi:10.1128/AEM.03299-15 (2016).
31 Kandel, P. P., Almeida, R. P. P., Cobine, P. A. & De La Fuente, L. Natural competence rates are variable among *Xylella fastidiosa* strains and homologous recombination occurs in vitro between

549 subspecies *fastidiosa* and *multiplex*. *Mol Plant Microbe Interact* **30**, 589-600, doi:10.1094/MPMI-
550 02-17-0053-R (2017).
551 32 Kung, S. H. & Almeida, R. P. P. Biological and genetic factors regulating natural competence in a
552 bacterial plant pathogen. *Microbiology* **160**, 37-46, doi:10.1099/mic.0.070581-0 (2014).
553 33 Kandel, P. P., Lopez, S. M., Almeida, R. P. P. & De La Fuente, L. Natural competence of *Xylella*
554 *fastidiosa* occurs at a high frequency inside microfluidic chambers mimicking the bacterium's
555 natural habitats. *Appl Environ Microbiol* **82**, 5269-5277, doi:10.1128/AEM.01412-16 (2016).
556 34 Nguyen, Y. *et al. Pseudomonas aeruginosa* minor pilins prime type IVa pilus assembly and promote
557 surface display of the PilY1 adhesin. *J Biol Chem* **290**, 601-611, doi:10.1074/jbc.M114.616904
558 (2015).
559 35 Jacobsen, T., Bardiaux, B., Francetic, O., Izadi-Pruneyre, N. & Nilges, M. Structure and function of
560 minor pilins of type IV pili. *Med Microbiol Immunol* **209**, 301-308, doi:10.1007/s00430-019-00642-
561 5 (2020).
562 36 Giltner, C. L., Nguyen, Y. & Burrows, L. L. Type IV pilin proteins: versatile molecular modules.
563 *Microbiol Mol Biol Rev* **76**, 740-772, doi:10.1128/MMBR.00035-12 (2012).
564 37 Kandel, P. P., Chen, H. & De La Fuente, L. A short protocol for gene knockout and complementation
565 in *Xylella fastidiosa* shows that one of the type IV pilin paralogs (PD1926) is needed for twitching
566 while another (PD1924) affects pilus number and location. *Appl Environ Microbiol* **84**, e01167-
567 01118 (2018).
568 38 Burrows, L. L. *Pseudomonas aeruginosa* twitching motility: type IV pili in action. *Annu Rev Microbiol*
569 **66**, 493-520, doi:10.1146/annurev-micro-092611-150055 (2012).
570 39 Nolan, L. M. *et al. Pseudomonas aeruginosa* is capable of natural transformation in biofilms.
571 *Microbiology* **166**, 995-1003, doi:10.1099/mic.0.000956 (2020).
572 40 Matsumoto, A., Young, G. M. & Igo, M. M. Chromosome-based genetic complementation system
573 for *Xylella fastidiosa*. *Appl Environ Microbiol* **75**, 1679-1687, doi:10.1128/AEM.00024-09 (2009).
574 41 Galvani, C. D., Li, Y., Burr, T. J. & Hoch, H. C. Twitching motility among pathogenic *Xylella*
575 *fastidiosa* isolates and the influence of bovine serum albumin on twitching-dependent colony fringe
576 morphology. *FEMS Microbiol Lett* **268**, 202-208, doi:10.1111/j.1574-6968.2007.00601.x (2007).
577 42 Meng, Y. *et al.* Upstream migration of *Xylella fastidiosa* via pilus-driven twitching motility. *J Bacteriol*
578 **187**, 5560-5567, doi:10.1128/JB.187.16.5560-5567.2005 (2005).
579 43 Cehovin, A. *et al.* Specific DNA recognition mediated by a type IV pilin. *Proc Natl Acad Sci U S A*
580 **110**, 3065-3070, doi:10.1073/pnas.1218832110 (2013).
581 44 Salleh, M. Z. *et al.* Structure and properties of a natural competence-associated pilin suggest a
582 unique pilus tip-associated DNA receptor. *mBio* **10**, e00614-00619, doi:10.1128/mBio (2019).
583 45 Leong, C. G. *et al.* The role of core and accessory type IV pilus genes in natural transformation and
584 twitching motility in the bacterium *Acinetobacter baylyi*. *PLoS One* **12**, e0182139,
585 doi:10.1371/journal.pone.0182139 (2017).
586 46 Braus, S. A. G. *et al.* The molecular basis of FimT-mediated DNA uptake during bacterial natural
587 transformation. *Nature Communications* **13**, 1065, doi:10.1038/s41467-022-28690-1 (2022).
588 47 Aubry, S., Kelly, S., Kümpers, B. M., Smith-Unna, R. D. & Hibberd, J. M. Deep evolutionary
589 comparison of gene expression identifies parallel recruitment of *trans*-factors in two independent
590 origins of C4 photosynthesis. *PLoS Genet* **10**, e1004365, doi:10.1371/journal.pgen.1004365
591 (2014).
592 48 Jacques, M. A. *et al.* Using ecology, physiology, and genomics to understand host specificity in
593 *Xanthomonas*. *Annu Rev Phytopathol* **54**, 163-187, doi:10.1146/annurev-phyto-080615-100147
594 (2016).
595 49 Giltner, C. L., Rana, N., Lunardo, M. N., Hussain, A. Q. & Burrows, L. L. Evolutionary and functional
596 diversity of the *Pseudomonas* type IVa pilin island. *Environ Microbiol* **13**, 250-264,
597 doi:10.1111/j.1462-2920.2010.02327.x (2011).
598 50 van Schaik, E. J. *et al.* DNA binding: a novel function of *Pseudomonas aeruginosa* type IV pili. *J*
599 *Bacteriol* **187**, 1455-1464, doi:10.1128/JB.187.4.1455-1464.2005 (2005).
600 51 Laurenceau, R. *et al.* A type IV pilus mediates DNA binding during natural transformation in
601 *Streptococcus pneumoniae*. *PLoS Pathog* **9**, e1003473, doi:10.1371/journal.ppat.1003473 (2013).
602 52 Berry, J. L., Cehovin, A., McDowell, M. A., Lea, S. M. & Pelicic, V. Functional analysis of the
603 interdependence between DNA uptake sequence and its cognate ComP receptor during natural

transformation in *Neisseria* species. *PLoS Genet* **9**, e1004014, doi:10.1371/journal.pgen.1004014 (2013).

53 Vesel, N. & Blokesch, M. Pilus production in *Acinetobacter baumannii* is growth phase dependent and essential for natural transformation. *J Bacteriol* **203**, e00034- 00021, doi:10.1128/JB.00034-21 (2021).

54 Rumszauer, J., Schwarzenlander, C. & Averhoff, B. Identification, subcellular localization and functional interactions of PilMNOWQ and PilA4 involved in transformation competency and pilus biogenesis in the thermophilic bacterium *Thermus thermophilus* HB27. *FEBS J* **273**, 3261-3272, doi:10.1111/j.1742-4658.2006.05335.x (2006).

55 Carruthers, M. D. *et al.* Biological roles of nontypeable *Haemophilus influenzae* type IV pilus proteins encoded by the *pil* and *com* operons. *J Bacteriol* **194**, 1927-1933, doi:10.1128/JB.06540-11 (2012).

56 Tammam, S. *et al.* PilMNOPQ from the *Pseudomonas aeruginosa* type IV pilus system form a transenvelope protein interaction network that interacts with PilA. *J Bacteriol* **195**, 2126-2135, doi:10.1128/JB.00032-13 (2013).

57 Alm, R. A., Bodero, A. J., Free, P. D. & Mattick, J. S. Identification of a novel gene, *pilZ*, essential for type 4 fimbrial biogenesis in *Pseudomonas aeruginosa*. *J Bacteriol* **178**, 46-53 (1996).

58 Marko, V. A., Kilmury, S. L. N., MacNeil, L. T. & Burrows, L. L. *Pseudomonas aeruginosa* type IV minor pilins and PilY1 regulate virulence by modulating FimS-AlgR activity. *PLoS Pathog* **14**, e1007074, doi:10.1371/journal.ppat.1007074 (2018).

59 Ayers, M. *et al.* PilM/N/O/P proteins form an inner membrane complex that affects the stability of the *Pseudomonas aeruginosa* type IV pilus secretin. *J Mol Biol* **394**, 128-142, doi:10.1016/j.jmb.2009.09.034 (2009).

60 Li, Y. *et al.* Type I and type IV pili of *Xylella fastidiosa* affect twitching motility, biofilm formation and cell-cell aggregation. *Microbiology* **153**, 719-726, doi:10.1099/mic.0.2006/002311-0 (2007).

61 Drake, S. L., Sandstedt, S. A. & Koomey, M. PilP, a pilus biogenesis lipoprotein in *Neisseria gonorrhoeae*, affects expression of PilQ as a high-molecular-mass multimer. *Mol Microbiol* **23**, 657-668 (1997).

62 Hardy, L., Juan, P. A., Coupat-Goutaland, B. & Charpentier, X. Transposon insertion sequencing in a clinical isolate of *Legionella pneumophila* identifies essential genes and determinants of natural transformation. *J Bacteriol* **203**, e00548-00520 (2021).

63 D'Attoma, G. *et al.* Phenotypic characterization and transformation attempts reveal peculiar traits of *Xylella fastidiosa* subspecies *pauca* strain De Donno. *Microorganisms* **8**, 1832, doi:10.3390/microorganisms8111832 (2020).

64 Davis, M. J., French, W. J. & Schaad, N. W. Axenic culture of the bacteria associated with phony disease of peach and plum leaf scald. *Curr Microbiol* **6**, 309-314 (1981).

65 Cruz, L. F., Cobine, P. A. & De La Fuente, L. Calcium increases *Xylella fastidiosa* surface attachment, biofilm formation, and twitching motility. *Appl Environ Microbiol* **78**, 1321-1331, doi:10.1128/AEM.06501-11 (2012).

66 Gluck-Thaler, E. *et al.* Repeated gain and loss of a single gene modulates the evolution of vascular plant pathogen lifestyles. *Sci Adv* **6**, eabc4516 (2020).

67 Zhu, X. *et al.* Mitochondrial copper and phosphate transporter specificity was defined early in the evolution of eukaryotes. *Elife* **10**, e64690, doi:10.7554/eLife.64690 (2021).

68 Sheffield, P., Garrard, S. & Derewenda, Z. Overcoming expression and purification problems of RhoGDI using a family of “Parallel” expression vectors. *Protein Expr. Purif.* **15**, 34-39 (1999).

69 Schneider, C. A., Rasband, W. S. & Eliceiri, K. W. NIH Image to ImageJ: 25 years of image analysis. *Nat Methods* **9**, 671-675 (2012).

70 Simko, I. & Piepho, H.-P. The area under the disease progress stairs: Calculation, advantage, and application. *Phytopathology* **102**, 381-389 (2012).

71 Kelley, L. A., Mezulis, S., Yates, C. M., Wass, M. N. & Sternberg, M. J. E. The Phyre2 web portal for protein modeling, prediction and analysis. *Nat Protoc* **10**, 845-858, doi:10.1038/nprot.2015.053 (2015).

72 Di Tommaso, P. *et al.* T-Coffee: a web server for the multiple sequence alignment of protein and RNA sequences using structural information and homology extension. *Nucleic Acids Res* **39**, W13-17, doi:10.1093/nar/gkr245 (2011).

73 Katoh, K., Misawa, K., Kuma, K. & Miyata, T. MAFFT: a novel method for rapid multiple sequence alignment based on fast Fourier transform. *Nucleic Acids Res* **30**, 3059-3066 (2002).
74 Stamatakis, A. RAxML version 8: a tool for phylogenetic analysis and post-analysis of large phylogenies. *Bioinformatics* **30**, 1312-1313, doi:10.1093/bioinformatics/btu033 (2014).
75 Sauvage, T., Plouviez, S., Schmidt, W. E. & Fredericq, S. TREE2FASTA: a flexible Perl script for batch extraction of FASTA sequences from exploratory phylogenetic trees. *BMC Res Notes* **11**, 164, doi:10.1186/s13104-018-3268-y (2018).
76 Madeira, F. *et al.* The EMBL-EBI search and sequence analysis tools APIs in 2019. *Nucleic Acids Res* **47**, W636-W641, doi:10.1093/nar/gkz268 (2019).
77 Crooks, G. E., Hon, G., Chandonia, J. M. & Brenner, S. E. WebLogo: a sequence logo generator. *Genome Res* **14**, 1188-1190, doi:10.1101/gr.849004 (2004).
78 Ihaka, R. & Gentleman, R. R: A language for data analysis and graphics. *J. Comput. Graph. Stat.* **5**, 299-314 (1996).

Acknowledgments

We thank Dr. Michelle Mendonça Pena for helping with phylogenetic analyses. We thank the Alabama Supercomputing Authority for granting access to their high-performance computing platform. We acknowledge funding from Alabama Agricultural Experiment Station (AAES) Hatch Program (L.D., P.A.C., N.P) and Auburn Internal Grant Program.

Author contributions

M.V.M., P.A.C. and L.D.F. designed research; M.V.M., X.Z. D.S., L.M.G., E.N. and N.P. performed research; M.V.M., N.P., P.A.C. and L.D. analyzed data; and M.V.M. and L.D.F. wrote the paper.

Competing Interests statement

The authors declare no conflict of interest.

Figure legends

Fig. 1. Natural transformation and twitching motility phenotypes of *X. fastidiosa* mutant strains used in this study. Quantification of natural transformation was performed by enumerating total viable cells and recombinants and results are expressed as the ratio of recipient cells transformed (recombination frequency; values shown in the x-axis of the chart). Twitching motility was determined by spotting cells on agar plates and measuring the movement fringe width after 4 days of growth at 28 ºC (values shown in the y-axis of the chart). Results of mutant strains for paralogous genes are shown using the same color for text and symbol. The non-motile and non-recombinant mutants are shown as a black dot. The WT is represented as a dark blue triangle and all other mutants are represented as black triangles. Data represent means and standard errors. Different letters in parenthesis indicate significant difference in fringe width as analyzed by ANOVA followed by Tukey's HSD multiple comparisons of means ($P<0.05$; n = three to 14 independent replicates with eight to 48 internal replicates each). * and ** indicate significant difference ($P<0.05$ and $P<0.005$, respectively) of recombination frequency through natural competence in comparison to the WT as determined using Student's *t*-test (n = three to 21 independent replicates with two internal replicates each). The detection limit for recombination frequency was 10^{-7} and for twitching motility was 10 µm. Mutants below the detection limit are shown in the non-motile and non-recombinant group.

Fig. 2. FimT3 DNA binding activity. **a** Transmission electron microscopy micrographs of pilus formation by *X. fastidiosa* WT and Δ*fimT3* cells. Arrows are pointing to TFP. Similar events were captured in two independent experiments. Images were captured at 31,500× magnification. Scale bars, 500 nm. **b** Uptake of Cy-3-labeled pAX1-Cm plasmid into a DNaseI resistant state by *X. fastidiosa* cells observed using a fluorescent microscope. The images correspond to the bright field (left), Cy-3 channel (center) and merged images (right). In merged images, arrows are pointing to fluorescent DNA foci at the cell poles. Similar events were captured in three independent experiments. Images were captured at 100× magnification. Scale bars, 1.5 µm. **c** DNA-binding ability of purified FimT1s, FimT2s and FimT3s assessed by agarose EMSA. Similar events were captured in three independent experiments. **d** Surface

electrostatics representation of FimT3 merged with its ribbon representation. The arginine amino acid residues (R160 and R162) that were mutated for functional studies are highlighted in the figure. The electrostatic potential (eV) color scale is shown in the figure. **e** DNA-binding ability of purified FimT3s and FimT3s-R160AR162A assessed by agarose EMSA. Similar events were captured in three independent experiments. **f** Titration of the DNA binding activity of FimT3s and FimT3s-R160AR162A by native acrylamide EMSA. Similar events were captured in two independent experiments. **g** Densitometry analysis of the DNA binding activity of FimT3s and FimT3s-R160AR162A in acrylamide EMSA. The fluorescent intensity of the shifted DNA bands of Cy-3-labeled Km resistance cassette presented in **f** was measured using ImageJ. The fluorescent intensity of shifted bands when treated only with 1, 2, 5, and 10 μM of each protein was measured, since they presented higher shifts in electrophoretic mobility within this protein concentration range. **h** Area under the fluorescent curve. The area under the fluorescent curves in **g** was calculated to quantify the DNA-binding affinity of FimT3s and FimT3s-R160AR162A. Statistical significance was determined using Student's *t*-test (* indicates $P<0.05$ in comparison to the wild-type protein; n = two independent replicates).

Fig. 3. Phylogenetic tree based on nucleotide sequences of the three *fimT* paralogs from Xanthomonadaceae bacterial strains with whole-genome sequences available. The phylogenetic tree was built using the Maximum-likelihood method and visualized using FigTree. Branches with bootstrap values below 70% were collapsed, except where indicated. This was performed to keep conciseness of the figure while indicating the different clusters for *fimT1*, *fimT2* and *fimT3*. *X. fastidiosa* is highlighted in blue within the tree. When known, clade I *Xanthomonas* spp. are highlighted in orange, and clade II *Xanthomonas* spp. are highlighted in purple. Bacterial species encoding all three *fimT* paralogs are indicated in bold, while those encoding two paralogs are shown in italics and those encoding only one paralog are underlined within the tree. The order of appearance of bacterial species in collapsed branches follows the original order of appearance within the tree. For representation purposes, branches are highlighted by color according to each *fimT* paralog. Green: *fimT1*; Dark blue: *fimT2*; Red: *fimT3*. *** Indicates clusters within the *fimT3* clade which contain few FimT3 sequences with no GRxR motif (see Table S5 and Fig. S15). Abbreviations are the following. ***Coralloluteibacterium*:** Cst – *C. stylophorae*.

***Luteimonas*:** Lab – *L. abyssi*; Lae – *L. aestuarii*; Laq – *L. aquatica*; Lar – *L. arsenica*; Lch – *L. chenhongjianii*; Lcu – *L. cucumeris*; Lde – *L. deserti*; Lfr – *L. fraxinea*; Lgi – *L. gilva*; Lgr – *L. granuli*; Lhu – *L. huabeiensis*; Llu – *L. lumbrici*; Lma – *L. marina*; Lme – *L. mephitis*; Lpd – *L. padinae*; Lpn – *L. panaciterrae*; Lsp – *L.* sp.; Lte – *L. terrae*; Lti – *L. terricola*; Lwe – *L. wenzhouensis*; Lyi – *L. yindakuii*. ***Lysobacter*:** Lys – *L.* sp. ***Pseudoxanthomonas*:** Pbe – *P. beigongshangi*; Pbr – *P. broegbernensis*; Pco – *P. composti*; Pda – *P. daejeonensis*; Pdo – *P. dokdonensis*; Pge – *P. gei*; Phe – *P. helianthi*; Pin – *P. indica*; Pja – *P. japonensis*; Pji – *P. jiangjuensis*; Pkl – *P. kalamensis*; Pko – *P. kaohsiungensis*; Pkr – *P. koreensis*; Pme – *P. mexicana*; Psc – *P. sacheonensis*; Psn – *P. sangjuensis*; Psp – *P.* sp.; Psx – *P. spadix*; Psu – *P. suwonensis*; Ptw – *P. taiwanensis*; Pwi – *P. winnipegensis*; Pwu – *P. wuyuanensis*; Pye – *P. yeongjuensis*. ***Rehaibacterium*:** Rte – *R. terrae*. ***Silanimonas*:** Sle – *S. lenta*. ***Stenotrophomonas*:** Sac – *S. acidaminiphila*; Sbe – *S. bentonitica*; Sch – *S. chelatiphaga*; Scy – *S. cyclobalanopsidis*; Sda – *S. daejeonensis*; Sge – *S. geniculata*; Sgi – *S. ginsengisoli*; Shu – *S. humi*; Sin – *S. indicatrix*; Skr – *S. koreensis*; Sla – *S. lactitubi*; Sma – *S. maltophilia*; Sne – *S. nematodicola*; Sni – *S. nitritireducens*; Spn – *S. panacihumi*; Spv – *S. pavanii*; Spi – *S. pictorum*; Srh – *S. rhizophila*; Sse – *S. sepilia*; Ssp – *S.* sp; Ste – *S. terrae*; Stu – *S. tumulicola*. ***Vulcaniibacterium*:** Vge – *V. gelatinicum*; Vte – *V. tengchongense*; Vth – *V. thermophilum*. ***Xanthomonas*:** Xab – *X. albilineans*; Xaf – *X. alfalfae*; Xar – *X. arboricola*; Xax – *X. axonopodis*; Xbr – *X. bromi*; Xcm – *X. campestris*; Xcn – *X. cannabis*; Xcs – *X. cassavae*; Xci – *X. cissicola*; Xct – *X. citri*; Xco – *X. codiaei*; Xcu – *X. curcubitae*; Xdy – *X. dyei*; Xer – *X. euroxanthea*; Xeu – *X. euvesicatoria*; Xfl – *X. floridensis*; Xfr – *X. fragariae*; Xho – *X. hortorum*; Xha – *X. hyacinthi*; Xhd – *X. hydrangea*; Xml – *X. maliensis*; Xms – *X. massiliensis*; Xme – *X. melonis*; Xna – *X. nasturtii*; Xor – *X. oryzae*; Xpe – *X. perforans*; Xpi – *X. pisi*; Xpo – *X. populi*; Xpr – *X. prunicola*; Xsa – *X. sacchari*; Xso – *X. sontii*; Xsp – *X.* sp.; Xth – *X. theicola*; Xtr – *X. translucens*; Xva – *X. vasicola*; Xve – *X. vesicatoria*. ***Xylella*:** Xtw – *X. taiwanensis*.

Fig. 4. Schematic representation of the functional role of TFP molecular components in natural competence and twitching motility of *X. fastidiosa*. The figure shows the structure of a type IV pilus (PilA1, PilA2 and PilA3), the alignment subcomplex (PilM, PilN, PilO and PilP), the inner membrane motor subcomplex (PilB, PilC, PilD, PilT and PilU), the pore subcomplex (PilF and PilQ), minor pilins (PilE1,

770 PilE2, PilV1, PilV2, PilW1, PilW2, PilX1, PilX2, FimT1, FimT2 and FimT3), TFP tip adhesins (PilY1-1,
771 PilY1-2 and PilY1-3), as well as regulatory proteins (PilG, PilH, PilI, PilJ, PilL, PilR, PilS, PilZ, ChpB and
772 ChpC). Proteins in the figure are color-coded according to their phenotype upon knockout mutation and
773 thus functional role. More information about the role of each protein is described in Table S1, throughout
774 the manuscript and in SI Discussion. OM – outer membrane; P – periplasm; IM – inner membrane.
775

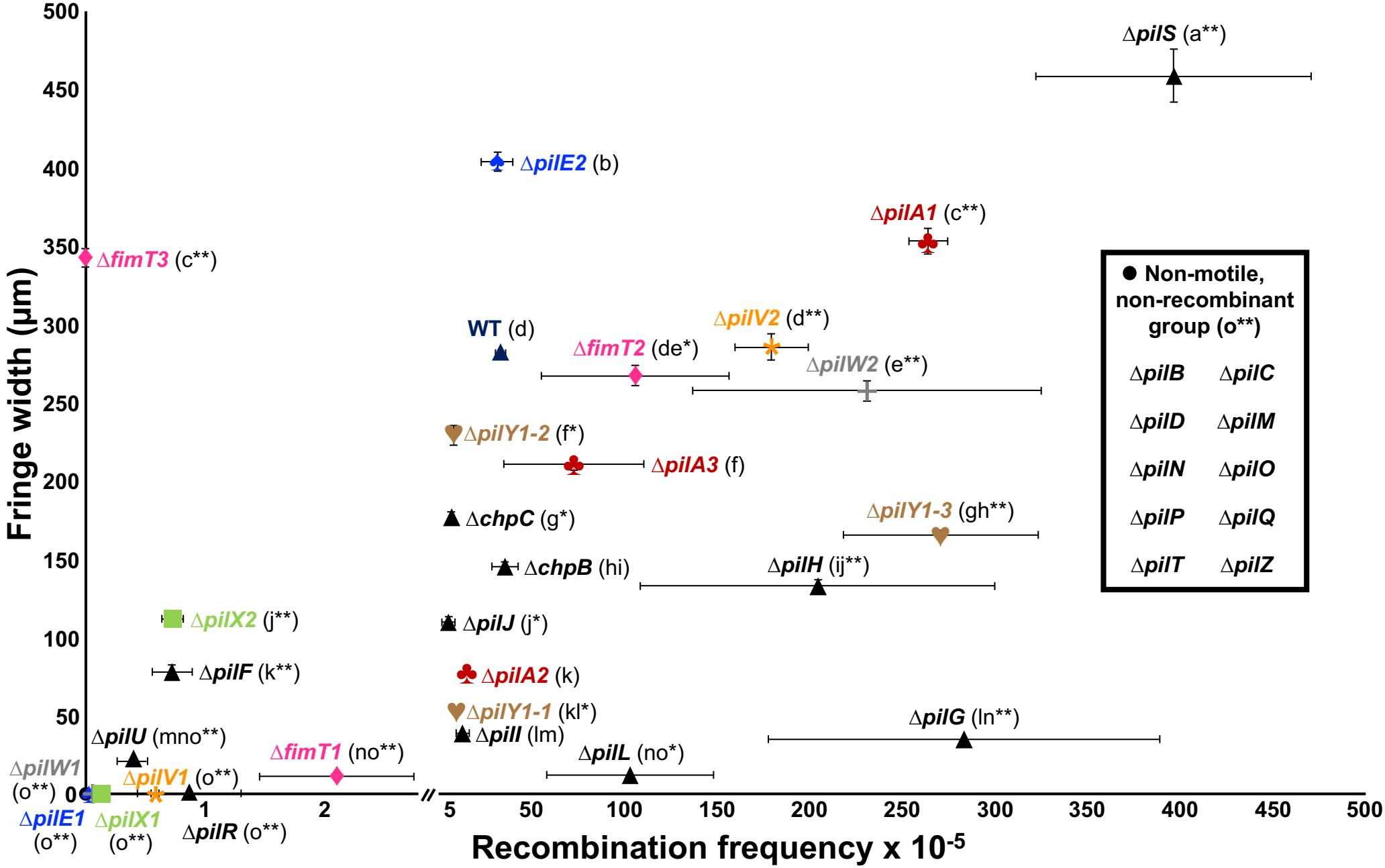
Fringe width (µm)
500
450
400
350
300
250
200
150
100
50
0
ΔpilS (a**)
ΔpilE2 (b)
ΔpilA1 (c**)
ΔfimT3 (c**)
WT (d)
ΔpilV2 (d**)
ΔfimT2 (de*)
ΔpilW2 (e**)
ΔpilY1-2 (f*)
ΔpilA3 (f)
ΔchpC (g*)
ΔpilY1-3 (gh**)
ΔchpB (hi)
ΔpilH (ij**)
ΔpilX2 (j**)
ΔpilJ (j*)
ΔpilF (k**)
ΔpilA2 (k)
ΔpilY1-1 (kl*)
ΔpilI (lm)
ΔpilG (ln**)
ΔpilU (mno**)
ΔfimT1 (no**)
ΔpilL (no*)
ΔpilW1 (o**)
ΔpilV1 (o**)
ΔpilE1 (o**)
ΔpilX1 (o**)
ΔpilR (o**)
1
2
5
50
100
150
200
250
300
350
400
450
500
Recombination frequency x 10-5
● Non-motile, non-recombinant group (o**)
ΔpilB ΔpilC
ΔpilD ΔpilM
ΔpilN ΔpilO
ΔpilP ΔpilQ
ΔpilT ΔpilZ

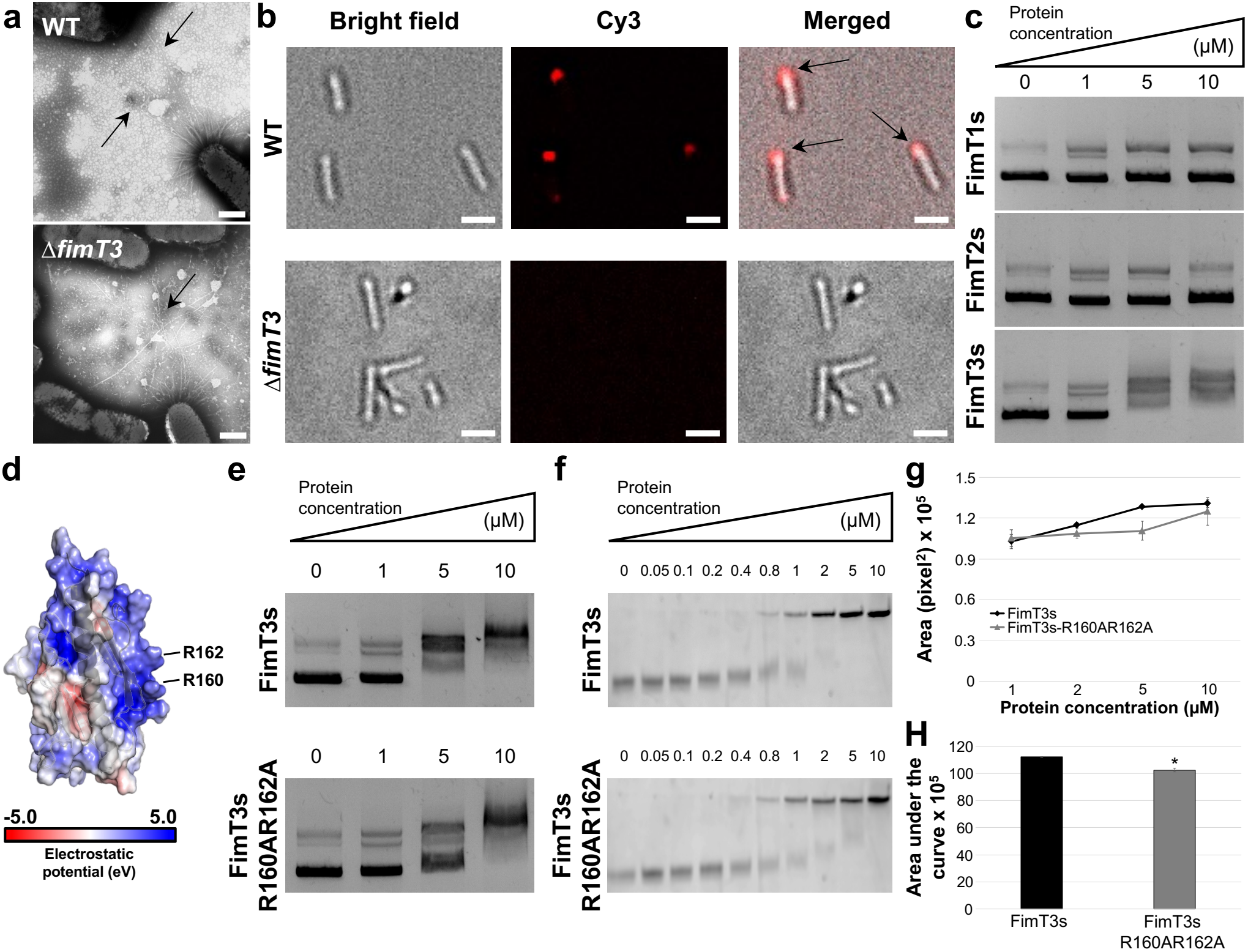
a
WT
ΔfimT3
b
Bright field
Cy3
Merged
WT
ΔfimT3
c
Protein concentration (μM)
0 1 5 10
FimT1s
FimT2s
FimT3s
d
R162
R160
-5.0
5.0
Electrostatic potential (eV)
e
Protein concentration (μM)
0 1 5 10
FimT3s
FimT3s R160AR162A
f
Protein concentration (μM)
0 0.05 0.1 0.2 0.4 0.8 1 2 5 10
FimT3s
FimT3s R160AR162A
g
Area (pixel²) x 10⁵
1.5
1.2
0.9
0.6
0.3
0
FimT3s
FimT3s-R160AR162A
1 2 5 10
Protein concentration (μM)
H
Area under the curve x 10⁵
120
100
80
60
40
20
0
*
FimT3s
FimT3s R160AR162A

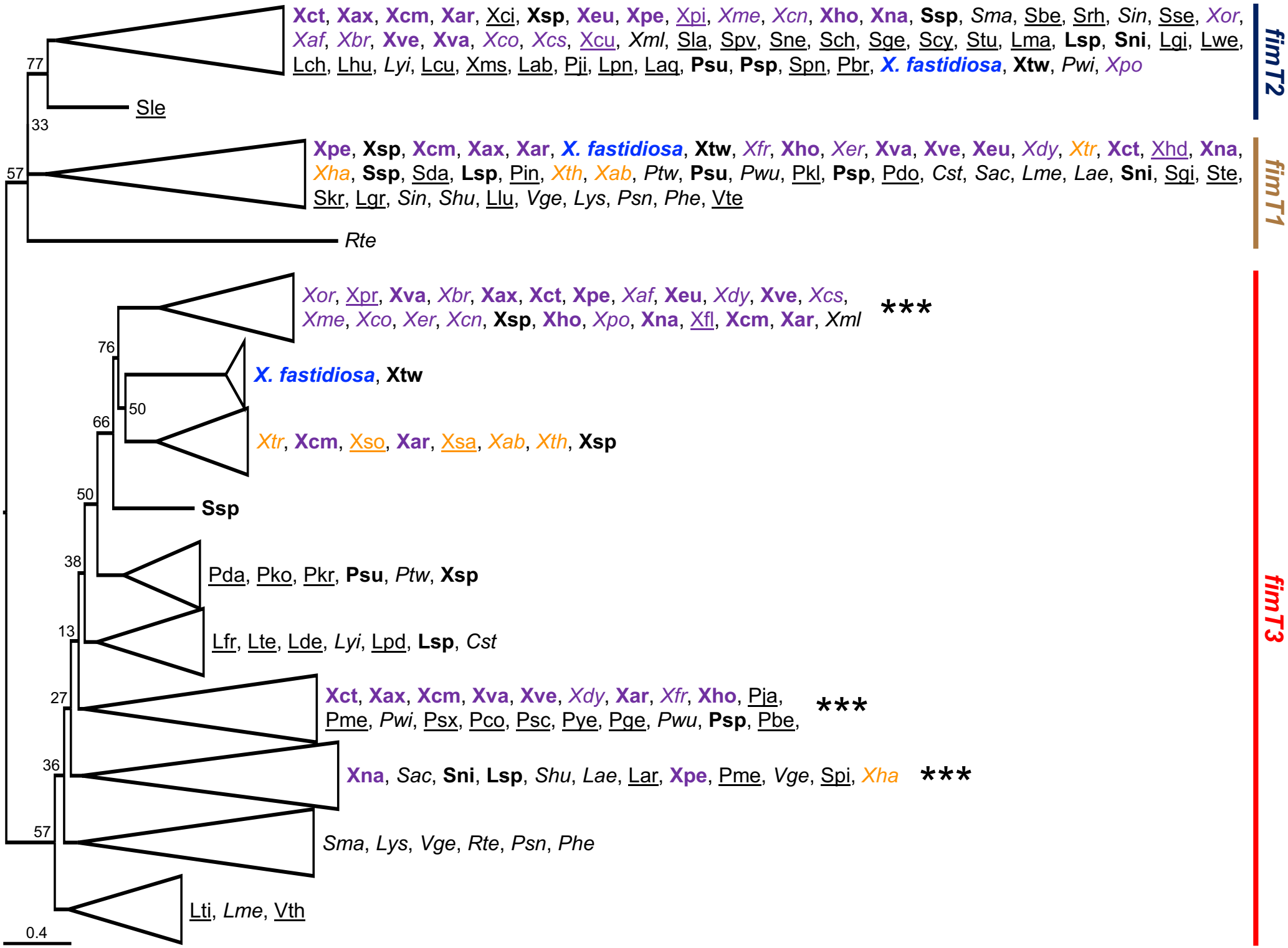
Xct, Xax, Xcm, Xar, Xci, Xsp, Xeu, Xpe, Xpi, Xme, Xcn, Xho, Xna, Ssp, Sma, Sbe, Srh, Sin, Sse, Xor, Xaf, Xbr, Xve, Xva, Xco, Xcs, Xcu, Xml, Sla, Spv, Sne, Sch, Sge, Scy, Stu, Lma, Lsp, Sni, Lgi, Lwe, Lch, Lhu, Lyi, Lcu, Xms, Lab, Pji, Lpn, Laq, Psu, Psp, Spn, Pbr, X. fastidiosa, Xtw, Pwi, Xpo
Sle
Xpe, Xsp, Xcm, Xax, Xar, X. fastidiosa, Xtw, Xfr, Xho, Xer, Xva, Xve, Xeu, Xdy, Xtr, Xct, Xhd, Xna, Xha, Ssp, Sda, Lsp, Pin, Xth, Xab, Ptw, Psu, Pwu, Pkl, Psp, Pdo, Cst, Sac, Lme, Lae, Sni, Sgi, Ste, Skr, Lgr, Sin, Shu, Llu, Vge, Lys, Psn, Phe, Vte
Rte
Xor, Xpr, Xva, Xbr, Xax, Xct, Xpe, Xaf, Xeu, Xdy, Xve, Xcs, Xme, Xco, Xer, Xcn, Xsp, Xho, Xpo, Xna, Xfl, Xcm, Xar, Xml
***
X. fastidiosa, Xtw
Xtr, Xcm, Xso, Xar, Xsa, Xab, Xth, Xsp
Ssp
Pda, Pko, Pkr, Psu, Ptw, Xsp
Lfr, Lte, Lde, Lyi, Lpd, Lsp, Cst
Xct, Xax, Xcm, Xva, Xve, Xdy, Xar, Xfr, Xho, Pja, Pme, Pwi, Psx, Pco, Psc, Pye, Pge, Pwu, Psp, Pbe,
***
Xna, Sac, Sni, Lsp, Shu, Lae, Lar, Xpe, Pme, Vge, Spi, Xha
***
Sma, Lys, Vge, Rte, Psn, Phe
Lti, Lme, Vth
77
33
57
76
50
66
50
38
13
27
36
57
0.4
fimT2
fimT1
fimT3

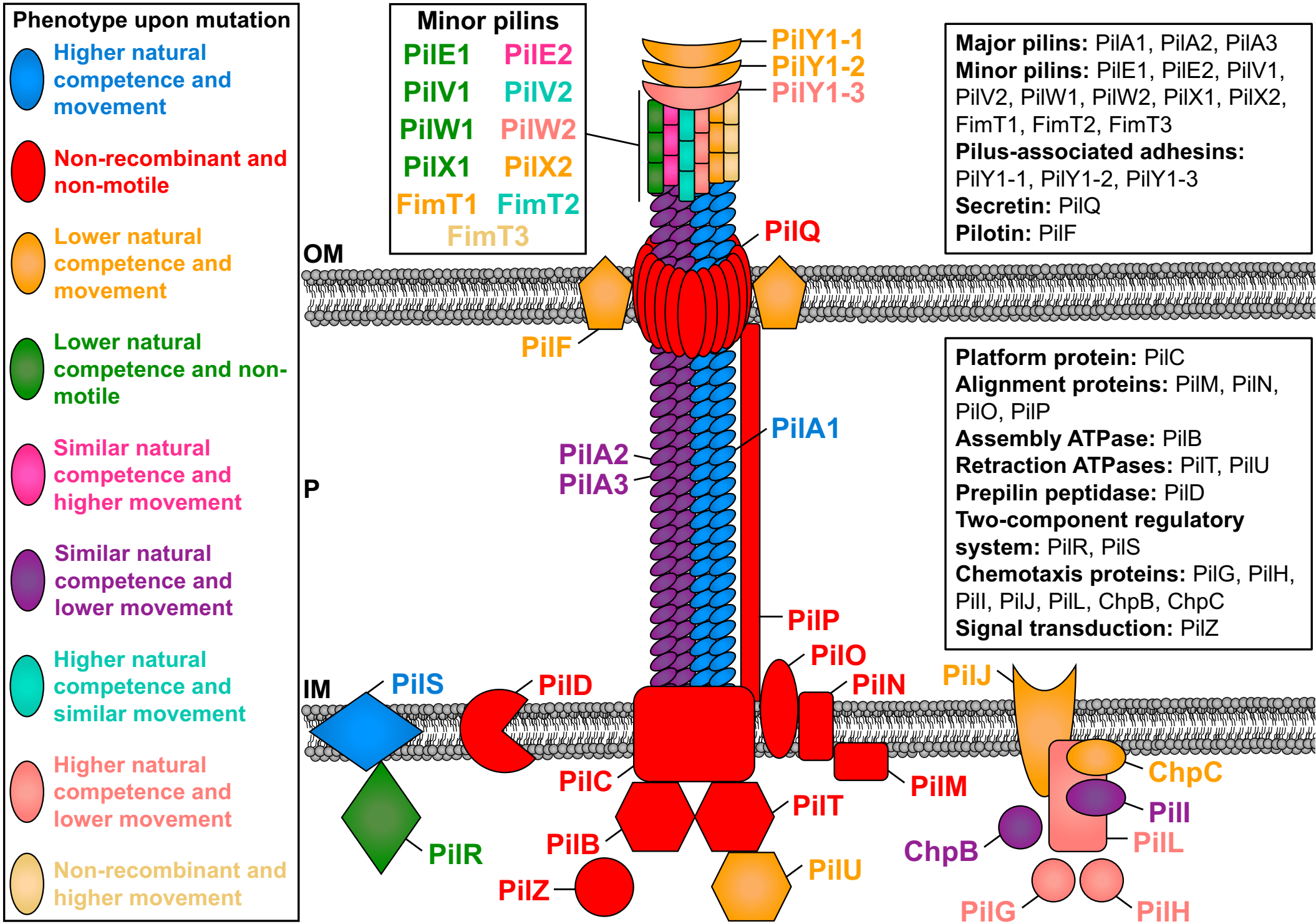
Phenotype upon mutation
Higher natural competence and movement
Non-recombinant and non-motile
Lower natural competence and movement
Lower natural competence and non-motile
Similar natural competence and higher movement
Similar natural competence and lower movement
Higher natural competence and similar movement
Higher natural competence and lower movement
Non-recombinant and higher movement
Minor pilins
PilE1 PilE2
PilV1 PilV2
PilW1 PilW2
PilX1 PilX2
FimT1 FimT2
FimT3
PilY1-1
PilY1-2
PilY1-3
Major pilins: PilA1, PilA2, PilA3
Minor pilins: PilE1, PilE2, PilV1, PilV2, PilW1, PilW2, PilX1, PilX2, FimT1, FimT2, FimT3
Pilus-associated adhesins: PilY1-1, PilY1-2, PilY1-3
Secretin: PilQ
Pilotin: PilF
OM
PilQ
PilF
PilA1
PilA2
PilA3
P
Platform protein: PilC
Alignment proteins: PilM, PilN, PilO, PilP
Assembly ATPase: PilB
Retraction ATPases: PilT, PilU
Prepilin peptidase: PilD
Two-component regulatory system: PilR, PilS
Chemotaxis proteins: PilG, PilH, PilI, PilJ, PilL, ChpB, ChpC
Signal transduction: PilZ
PilP
PilO
PilN
IM
PilS
PilD
PilJ
PilC
PilM
ChpC
PilT
PilI
PilR
PilB
ChpB
PilL
PilU
PilZ
PilG
PilH